 doi:10.20944/preprints202103.0330.v1

Article

EndoScreen Chip: serum complement C9 immunoassays improve risk prediction and early diagnosis of esophageal adenocarcinoma

Julie A. Webster[1], Alain Wuethrich[2], Karthik B. Shanmugasundaram[2], Renee S. Richards[1], Wioleta M. Zelek[3], Alok K. Shah[1], Louisa Gordon[1], Bradley J. Kendall[1,4,6], Gunter Hartel[1], B. Paul Morgan[3], Matt Trau[2,5] and Michelle. M. Hill[1,4]*

[1] QIMR Berghofer Medical Research Institute, Herston, QLD, Australia; websterjulie72@gmail.com; Renee.Richards@qimrberghofer.edu.au; akshahpharma@gmail.com; Louisa.Gordon@qimrberghofer.edu.au; Gunter.Hartel@qimrberghofer.edu.au; michelle.hill@qimrberghofer.edu.au
[2] Centre for Personalised Nanomedicine, Australian Institute for Bioengineering and Nanotechnology (AIBN), The University of Queensland, St Lucia, QLD, Australia; a.wuethrich@uq.edu.au; k.shanmugasundaram@uq.edu.au; m.trau@uq.edu.au
[3] Division of Infection and Immunity, Cardiff University, Heath Park, Cardiff United Kingdom; ZelekW@cardiff.ac.uk; morganbp@cardiff.ac.uk
[4] Faculty of Medicine, The University of Queensland, Herston, QLD, Australia; bradley.kendall@uq.edu.au
[5] School of Chemistry and Molecular Biosciences, The University of Queensland, St Lucia, QLD Australia;
[6] Department of Gastroenterolgy and Hepatology, Princess Alexandra Hospital, QLD Australia
* Correspondence: michelle.hill@qimrberghofer.edu.au; m.hill2@uq.edu.au

Simple Summary: Esophageal adenocarcinoma (EAC) is often detected at late stages and has a poor survival rate. The current diagnostic endoscopy-biopsy procedure is invasive and patients are selected for endoscopy based on clinical risk factors such as the precursor condition Barrett's esophagus, history of heartburn/reflux and high body mass index. To test the hypothesis that use of blood biomarkers can improve EAC risk prediction and diagnosis, we developed new immunoassays to measure complement C9 and a glycosylated form of C9, which we discovered as a novel biomarker for early stage EAC. In the current study population, use of the new blood biomarker test improved EAC prediction compared to clinical risk factors alone, indicating that a simple blood test can help the physician prioritize patients for endoscopic evaluation. Further development of a blood marker panel may enable population screening and early diagnosis of EAC, thereby reduce mortality from this cancer.

Abstract: Esophageal adenocarcinoma (EAC) detection relies on endoscopy-biopsy diagnosis, with routine endoscopic surveillance recommended for Barrett's esophagus (BE) patients. Here, we examine the utility of blood biomarkers in patient risk stratification by translating the EAC blood biomarker Jacalin lectin binding complement C9 (JAC-C9) into a novel microfluidic immunoassay, the EndoScreen Chip. Cohort evaluation (n=46) showed elevated serum total C9 and JAC-C9 in EAC. Logistic regression modeling demonstrated that addition of C9 and JAC-C9 to patient risk factors (age, body mass index and heartburn/reflux history) improved EAC prediction from AUROC of 0.838 to 0.931. Serum JAC-C9 strongly predicted EAC (vs BE OR= 4.6, 95% CI: 1.6-15.6, p = 0.014; vs Healthy OR=4.1, 95% CI:1.2-13.7, p = 0.024) while total C9 was moderately predictive for BE (vs EAC OR=1.4; 95% CI: 1.0-1.8, p = 0.032; vs Healthy OR=0.8; 95% CI: 0.6-1.0, p = 0.039). This translational study demonstrates the potential utility of blood biomarkers in improving triaging for diagnostic endoscopy.

Keywords: Barrett's esophagus; biomarker; surveillance; screening; surface-enhanced Raman spectroscopy; SERS; complement component; liquid biopsy; lectin; glycoprotein.

 doi:10.20944/preprints202103.0330.v1

1. Introduction

Implementation of population screening programs for breast and cervical cancers have successfully reduced mortality by detecting these cancers at an earlier stage, motivating the development of similar programs for other cancers. An effective cancer screening program is predicated on the identification of a defined high-risk population and the availability of a sensitive, cost-effective, minimally invasive screening test. In this work, we aim to translate serum biomarkers for early stage esophageal adenocarcinoma (EAC) into a blood test to better stratify patients for the gold standard diagnosis by upper endoscopy-biopsy, an invasive, costly and time-consuming procedure unsuitable for population screening [1].

EAC is thought to develop as a consequence of chronic gastro-esophageal reflux disease (GERD), with the metaplastic condition Barrett's esophagus (BE) being the only known precursor condition [2,3]. To detect EAC at an early stage, BE patients and those with multiple risk factors for BE and EAC, such as age > 50 years, male sex, GERD history, acid suppression medication and high body mass index (BMI) are recommended to undergo endoscopic screening [4-8]. Despite improved risk factor identification and a BE surveillance program, temporal epidemiological data show that there has been no change in the proportion of people diagnosed into each stage of EAC since the 1970s [9]. Patients with EAC face a poor prognosis, with 5-year survival of less than 20% [10,11]. Detection at an early stage significantly improves survival, exemplified by the 48% 5-year survival rate for localized EAC [11]. Hence, there is an urgent need to improve early EAC risk stratification and diagnosis.

Several novel cytology sampling methods and biomarkers for detection of BE are at late stages of clinical development, including CytoSponge, EsophaCap and EsoCheck [2,12]. For BE patients who have undergone endoscopy with biopsy, TissueCypher and BarreGEN predicts EAC risk using a 15-marker immunohistochemistry panel and gene mutational load, respectively [2]. While these tests will assist BE diagnosis and risk stratification, >90% of EAC patients do not have prior diagnosis of BE [11]. Therefore, there is an unmet need for biomarkers that detect EAC and high grade dysplastic (HGD) BE in a high-risk population.

Based on the role of glycosylation in carcinogenesis, and the reported glycan changes during BE progression to EAC [13], we embarked on a glycoproteomics program to discover serum glycoprotein biomarkers for early EAC. Our pipeline used a panel of naturally occurring glycan-binding proteins, lectins, as affinity agents for different glycoforms [14], and tandem mass spectrometry methods for protein identification and quantitation [15]. Through a phased biomarker program with 4 patient cohorts from Australia and the USA (n>350), we discovered and validated a panel of serum glycoproteins that can detect early EAC, at the HGD stage [15,16]. To begin translating our biomarker panel into immunoassays for clinical use, we first focused on the most robust biomarker candidate, complement component C9 (C9). C9 is a glycoprotein of the terminal complement pathway, which functions to induce cytotoxicity by forming the membrane attack complex on target cell membranes. Our glycoproteomics studies confirmed elevated levels of 4 different circulating C9 glycoforms that bind to AAL, EPHA, JAC and NPL lectins, respectively [15,16]. In addition, we detected strong staining of C9 protein in dysplastic BE and EAC tissues by immunohistochemistry [16], although we were not able to distinguish glycoforms on tissue.

Given the need for a non-invasive EAC test suitable for screening, we developed two new immunoassays in this study; a traditional enzyme-linked immunosorbent assay (ELISA) for total C9 concentration in the serum, and a microfluidic immunoassay, the EndoScreen Chip, that uses surface-enhanced Raman spectroscopy (SERS) for the analysis of JAC lectin-binding C9 (JAC-C9). The performance of each immunoassay was compared to gold standard endoscopy-biopsy diagnosis in a cohort of 46 participants. The diagnostic value of the blood biomarker panel was then evaluated in multimodal logistic regression models.

 doi:10.20944/preprints202103.0330.v1

2. Materials and Methods

2.1. Study Cohort and Experimental Design

The study was approved by the Human Research Ethics Committee of QIMR Berghofer Medical Research Institute. A subset of the previously analyzed serum samples [15] were selected based on sample availability and were originally selected from the Study for Digestive Health [17,18]. All selected participants were male and were matched on the basis of age. Patient categorization into healthy, BE or EAC was confirmed histologically. Serum was taken at the time of endoscopic sample collection. Healthy controls had no history of esophageal cancer and no evidence of esophageal histological abnormality at the time of sample collection. Supplementary table I describes the characteristics of the cohort.

For analysis of serum C9 by ELISA, the samples were randomized across the ELISA plates. For analysis of JAC-C9 in serum, samples were analyzed blindly in conducting the assay. Method of modelling was determined prior to experimental analysis.

2.2. Recombinant Protein Expression and Purification

A human embryonic kidney 293 (Hek293) cell line stably expressing His-human C9 was generated using a human C9 pSectag2a plasmid kindly provided by Associate Professor Michelle Dunstone (Monash University) [19]. Hek293 cells were maintained in DMEM/Nutrient Mixture F-12 Ham (Sigma) in 2.5% heat inactivated fetal bovine serum (Gibco). C9-expressing Hek293 cells were seeded into HYPERFlask ® (Corning) and cultured until 90% confluent. Media was replaced with DMEM/F12 containing 5 mL Hank's buffered saline, 1x ITS (insulin-transferrin-sodium selenite) (Sigma) and 3 μM sodium butyrate and cells were allowed to secrete protein for 3 days.

His-C9 was purified from collected culture media using an AKTA fast protein liquid chromatography (FPLC) with HisTrap excel 5 mL columns (GE Healthcare Life Sciences). Columns were equilibrated using 20 mM sodium phosphate/ 0.5 M sodium chloride; washed using 20 mM sodium phosphate/ 0.5 M sodium chloride/ 20 mM imidazole; and eluted using 20 mM sodium phosphate/ 0.5 M sodium chloride / 500 mM imidazole. Fractions containing protein were identified using a Bradford assay (Bio-Rad), pooled and dialyzed using 3.5K MWCO snakeskin dialysis tubing (Thermofisher Scientific) against 3 L of phosphate buffered saline (pH 7.4), replaced three times for 24 hours. Protein expression was confirmed using western blot and protein concentration was determined using SDS-PAGE with colloidal Coomassie using a bovine serum albumin (BSA) standard, and then verified again by nanodrop.

2.3. Antibody production and purification

Mouse monoclonal antibody (mAb) to human C9 was generated by immunization of wild type mice C57BL/6J, bred in house) with human C9 using standard schedules [20]. Immunized mice were screened for antibody responses by enzyme-linked immunosorbent assay (ELISA) and mice with the highest titre response were selected and reboosted before sacrificing and harvesting of spleens. The splenocytes were fused with SP2 myeloma and aliquots were placed in 96-well plates. Positive hybridomas were selected by direct ELISA on immobilized human C9. The C9-positive mAb secreting clones were subcloned by limiting dilution to monoclonality. Three sub-clones of clone 26 were expanded: 2G6, 3C9 and 4G2, from which 3C9 was chosen for characterization and cultured in an Integra bioreactor (Sigma Aldrich #Z688029-3EA) for large scale production of antibody.

Preprints (www.preprints.org) | NOT PEER-REVIEWED | Posted: 12 March 2021 doi:10.20944/preprints202103.0330.v1

The mAb was purified using 5ml HiTrap Protein G sepharose columns (GE Healthcare, #GE17-0405-01). The column was washed, equilibrated with phosphate buffered saline (PBS), then IgG-containing Integra supernatant was applied at 1-2 ml/min, the column washed with 50ml PBS, and bound antibody eluted with 5ml 0.1M glycine pH2.5, collecting 1ml fractions into 100µl 0.1M Tris pH 7.2. Peak fractions were identified, pooled and dialysed overnight at 4°C into PBS. Antibody concentration was measured using Bicinchonic Acid (BCA) assay and the purified IgG was stored frozen in aliquots at >1mg/ml. Mouse mAb was isotyped using IsoStrips (# 11493027001; Roche) as IgG1, *K*.

2.4. Serum purified C9 and production of depleted serum

C9-depleted serum and purified C9 standard were generated using affinity chromatography. Human serum was obtained from the Australian Red Cross Blood Service under QIMRB human ethics approval P2352. Serum from five healthy donors was pooled, diluted 1:1 with PBS then sterile filtered (0.22µm). A 20ml sample of the pooled serum was injected onto a 1ml PBS-equilibrated HiTrap NHS-Activated HP affinity column (Cytiva) coupled to a monoclonal anti-C9 antibody [21]. C9-depleted serum fractions were collected in the flow-through and depletion confirmed by ELISA before pooling. The column was thoroughly washed with PBS before C9 was eluted with 5ml of 0.1M glycine, pH 2.5 and 4eutralized by addition of 0.5ml 1.5M Tris, pH 8.8. Eluted C9 was desalted and buffer exchanged vs PBS using a Zeba 7K MWCO spin desalting column (Thermofisher Scientific) and concentrated using an Amicon ultra 10K MWCO centrifugal filiter unit (Merck Millipore). C9 purity was assessed by SDS-PAGE and Western blot using a commercial anti-C9 antibody (ab17931, Abcam). Protein concentration of serum purified C9 was determined by BCA assay (Thermofisher Scientific).

2.5. Characterization of mAb 26 by Western blot

Human C9 (in house; 0.5µg) was placed in wells and resolved on 4–20% sodium dodecyl sulphate–polyacrylamide gel electrophoresis gels (#4561093; Biorad, Hemel Hempstead, UK) under reducing ® and non-reducing (NR) conditions, then electrophoretically transferred onto 0.45µm nitrocellulose membrane (GEHealthcare, Amersham, UK). After transfer, membranes were blocked with 5% BSA in PBS-T, washed in PBS-T, cut into strips and incubated overnight at 4°C with individual test sub-clone (2G6, 3C9, 4G2) each at 1µg/ml in 5% BSA PBS-T. Bound test mAb was detected by incubation with donkey anti-mouse IgG-HRP (Jackson ImmunoResearch, 715-035-150; 1: 10000 in 5% BSA PBS-T), developed with enhanced chemiluminescence (GE Healthcare) and visualized by autoradiography.

2.6. Hemolytic assay

To test the function of purified C9, protein was added back to C9-depleted serum at various doses up to 70µg/ml in undiluted C9-depleted serum (from the mAb 26 affinity column), then tested in hemolytic assay. Antibody-sensitized sheep erythrocytes (ShE; #ORLC25, Amboceptor Siemens, Dublin, Irleand) were suspended (2% vol:vol) in HEPES-buffered saline containing Ca^{2+} and Mg^{2+} (HBS^{++}). Aliquots (50µl) were placed into a 96-well round-bottomed plate followed by 50µl of the reconstituted C9-depleted serum diluted in HBS^{++}, then 50 µl of HBS^{++} [22]. C9-depleted serum or NHS were used as controls. Plates were incubated at 37°C for 30 min, centrifuged and hemoglobin in the supernatant measured by spectrophotometry (A405 nm). Percentage lysis was calculated according to: % Lysis= (A405 sample−A405 background)/(A405 max−A405 background)*100%.

2.7. C9 Direct ELISA

Preprints (www.preprints.org) | NOT PEER-REVIEWED | Posted: 12 March 2021 doi:10.20944/preprints202103.0330.v1

MaxiSorp™ ELISA plates (Sigma) were incubated overnight at 4°C with serum or eluate from the C9 pull-down diluted in sodium carbonate buffer (pH 9). Known concentrations of purified recombinant His C9 were used as control standard. The following day plates were washed three times with PBS-T. Mouse anti-C9 antibody was biotinylated using Biotin (Type B; Fast Conjugation kit, Abcam) following manufacturer's procedures. The plates were then incubated with 50 µL of biotinylated mouse anti-C9 antibody diluted in PBS-T/5% BSA (Sigma) at 2 µg/mL for 2 hours at room temperature. Plates were then washed three times with PBS-T, followed by 30 minutes incubation at room temperature with 100 µL of Streptavidin-HRP (Abcam) diluted 1/2500. Plates were washed four times with PBS- and developed using TMB (Thermofisher Scientific). When sufficient color was evident, development was stopped by adding 100 µL of 2M phosphoric acid (Sigma-Aldrich) and absorbance read at 450nm. The standard was calculated by (absorbance – background) then plotted against the known concentration. Concentration was determined by inputting (absorbance –background) into the linear regression formula and multiplied by dilution factor.

2.8. EndoScreen Chip Fabrication and Functionalization

The microfluidic device was fabricated using standard photolithography and according to a previous report [23]. Briefly, the EndoScreen Chip with an asymmetric electrode array was fabricated on a borosilicate glass substrate. The array consisted of 28 electrodes arranged in 4 rows to 7 electrodes each. The array of the asymmetric circular ring electrodes was designed using layout L-Edit V15 (Tanner Research, USA) and was written on 5-inch soda lime chrome mask (Shenzhen Qingyi, Singapore) using direct laser writer µPG 101 (Heidelberg Instruments, Australia). At first, the negative photoresist AZnLOF 2020 (Microchemicals GmbH, Germany) was coated on 4-inch borofloat glass wafer (Bonda Technology Pty Ltd, Singapore) for 30 s at 2000 rpm following a soft bake (2min, 110° C). The wafer was UV- exposed at 200 $mJcm^{-2}$ with the above patterned mask using a mask aligner (EVG 620, EV Group, Austria). After the post-exposure bake (1min, 110° C), the wafers were developed for 45 s in AZ726 MIF Developer (Microchemicals GmbH, Germany) and were cleaned using a PlasmaPro 80 (Oxford Instruments, UK) to remove photoresist residues. A thin layer of Ti (10 nm) and Au (200 nm) was deposited on to the wafers with a Temescal FC-2000 electron beam evaporator (Ferrotec, USA). Lift-off was then performed overnight in Remover PG (Microchemicals GmbH, Germany) at room temperature to reveal the gold coated circular microelectrode structures. In the second step, a well structure made of polydimethylsiloxane (PDMS) was prepared (wells of 6 mm diameter) that aligned with the electrode array. The PDMS was prepared by curing activated silicon elastomer solution (Sylgard® 184, Dow Midland, USA) for 1 h at 65 °C prior to thermal bonding of the PDMS structure on the electrode array.

The device was then functionalized by biotin-avidin chemistry (Supplementary Figure 2). First, 20 µL of 250 µg ml-1 biotin-BSA (Thermo Fisher Scientific, Australia) was incubated on the electrodes for 2 h followed by 20 µL of 100 µg/ml streptavidin (Thermo Fisher Scientific, Australia) and 20 µL of 100 µg/ml biotinylated-Jacalin (Vector Laboratories) were sequentially added to each well and incubated for 1 h at room temperature. The electrodes were thoroughly washed with 1 x PBS in-between each incubation step to remove any unbound biomolecules. Prior to the antigen incubation, 1% BSA in PBS was added to each well for 1 h as a blocking step.

2.9. SERS Nanotags Synthesis

The core sodium citrate coated gold nanoparticles (AuNPs) were synthesized according to the citrate synthesis by Frens [24] involving citrate reduction of gold (III) chloride trihydrate ($HAuCl_4$, Sigma-Aldrich, USA). Initially 100 ml HauCl4 solution was boiled in water (0.01% w/v) with the addition of 1 ml of 1% trisodium citrate dehydrate (Univar

Preprints (www.preprints.org) | NOT PEER-REVIEWED | Posted: 12 March 2021 doi:10.20944/preprints202103.0330.v1

solutions, USA) and under constant stirring for 20 min. Subsequently, 10 µL of 1 mM DTNB (5,5′-dithiobis (2- nitrobenzoic acid)) and 2 µL of 1 mM N-hydroxysuccinimide ester (DSP, Sigma Aldrich, USA) was added to 1ml of synthesized AuNPs and incubated at room temperature for 5 h with gentle shaking. After the incubation, the mixture was centrifuged at 5400 x g for 10 min and resuspended in 20 µL of 0.1 mM phosphate-buffered saline (PBS, pH 7.4) buffer. The PBS buffer containing the AuNPs conjugated Raman reporters was mixed with 500 µg of anti α-C9 antibody and incubated at room temperature for 30 min following a centrifugation at 600 x g for 6 min to remove unbound antibody. The SERS nanotags were then re-suspended in 0.1 % bovine serum albumin (BSA, Sigma Aldrich, USA).

2.10. C9 Sample Preparation for EndoScreen Chip Assay

Patient samples and C9 protein purified from human serum were denatured prior to use. The denaturation buffer was 40 mM Tris buffer (Thermo Fisher Scientific, USA) with 2 % of sodium dodecyl sulphate (Sigma-Aldrich, USA), 10 % of Triton buffer, and 40 mM dithiothreitol (Sigma-Aldrich, USA) in ultra-pure water. The denaturation buffer was added to the sample at volume ratio of 1:1 and was incubated at 65° C for 30 min. After denaturation, the mixture was alkylated by the addition of 1 M iodoacetamide (Bio-Rad laboratories, Canada) to make up a final concentration of approximately 100 mM and incubated for 30 min at ambient temperature and protected from light. The denatured patient samples were diluted 100-times in 1X PBS (pH 7.2) and stored at -20° C.

2.11. EndoScreen Chip Assay

Diluted samples (50 µL) was added to each well of the microfluidic device. The device was then connected to a signal generator 333510B (Agilent Technologies, Australia). Incubation of the sample was carried out under an applied alternating current electrohydrodynamics (ac-EHD) nanomixing (f=500Hz, Vpp=800 mV, t= 30 min) protocol that we have previously developed to improve detection specificity and sensitivity [23]. Next, the wells were washed with wash buffer (0.1% BSA, 0.01% Tween-20 in PBS) and incubated with 20 µL of SERS nanotags under the same ac-EHD conditions as above, but for 20 min. The wells were washed again with the wash buffer and the microfluidic device was stored at 4° C prior to the SERS mapping.

SERS mapping of the microfluidic device was performed by a WITec Alpha 300 R confocal Raman microscope with a HeNe laser (32 mW, 633 nm) with a 20 x microscopic objective. The acquisition parameters were 0.1 s integration time, step size of 1 µm, and mapping area was 60 µm x 60 µm (60 pixel × 60 pixel). Initial calibration for the instrument was performed by measuring the Raman intensity of the silicon substrate that produces a first-order photon peak at ~520 cm^{-1}. The raw Raman spectral data containing fluorescence and background noise were processed using a fifth-order polynomial fitting method developed by the Zhao and co-workers [25]. Each experiment was performed in triplicates and the intensity graph corresponding to the concentration of the C9 protein was plotted by taking the average of the peak Raman shift intensity of DTNB (1335 cm^{-1}).

2.12. Statistical Analysis

SDH cohort analyses were conducted in GraphPad Prism 8 and IBM SPSS Statistics 23. To adjust for normality, JAC-C9 Raman intensity was transformed using a natural log, then converted to z scores. BMI and heartburn/reflux history were entered as ordinal data into multinomial logistic regression based on increasing severity with population demographics [26]. Forced entry of BMI, age and heartburn/reflux history were used as the baseline/pre-test (model 1) of the multinomial logistic regression with the addition of

 doi:10.20944/preprints202103.0330.v1

serum JAC-C9 and total C9 (model 2), calculated using step-wise entry. All models were calculated relative to the healthy population or BE. Receiver operating characteristics (ROC) curves and confidence intervals were generated in JMP PRO (15.2.1, SAS Institute, Cary, NC, USA). For the positive predictive value, conversion from percentage points to percentages were calculated by the formula (percentage change/starting percentage) * 100%.

3. Results

3.1. Development and optimization of C9 ELISA

Immunoassays are highly reliable and cost-effective clinical tools used for the high throughput analysis of serum biomarkers; therefore, we aimed to establish and validate immunoassays for C9 and a specific glycoform of C9 that binds to Jacalin lectin (JAC-C9). Firstly, we developed renewable, quality reagents for the assays (Figure 1), including a new monoclonal anti-human-C9 antibody, m26 (Figure S1A, and S1B) and a recombinant C9 protein expressed in a mammalian cell system (Figures S1C and S1D). The antibody was verified to detect human recombinant and serum purified C9, with high affinity towards native C9 and a lower affinity towards denatured C9 (Figure S1E). In addition, we generated C9-depleted serum for use as background matrix in the immunoassay. Successful depletion was verified using a red blood cell lysis assay; depleted serum lowered lysis to near background, while add-back of C9 elevated lysis to level of normal human serum (Figure S1F).

Using recombinant His-C9 in the standard curve, the accuracy, repeatability, linearity and range of the C9 ELISA were assessed according to the US Food and Drug Administration Q2(R1) Validation Guidelines [27]. Firstly, the optimal serum dilution for measurement accuracy was determined using purified C9 spiked into C9-depleted serum at three concentrations (20 μg/mL, 40 μg/mL and 80 μg/mL). As shown in Figure 2A, at a serum dilution of 1/1250, the ELISA accurately measured the concentration of C9 in the spiked sample; however, at higher dilutions the ELISA underestimated the concentration of the spiked serum. Therefore, serum dilution was fixed at 1/1250. Repeatability was calculated following recommendations by Andreasson and colleagues [28]; co-efficient of variation (CV) was 3.8%, 5.6% and 4.3% for 20 μg/mL, 40 μg/mL and 80 μg/mL respectively (n=5). Linearity was used to demonstrate that the result obtained was directly proportional to the concentration. Given the accuracy of the 1/1250 dilution, it was clear that the result obtained was directly proportional to the concentration (Figure 2A); however, the linearity of the remaining concentrations were also assessed (Figure 2B) [28]. Despite the noted underestimate of concentration at high serum dilutions, the concentration determined was still proportional to the actual concentration. Furthermore, since the His-C9 standard was used in combination with spiked serum purified C9, these experiments demonstrate that recombinant His-C9 is a suitable alternative to serum purified C9 for use as an assay standard.

Preprints (www.preprints.org) | NOT PEER-REVIEWED | Posted: 12 March 2021 doi:10.20944/preprints202103.0330.v1

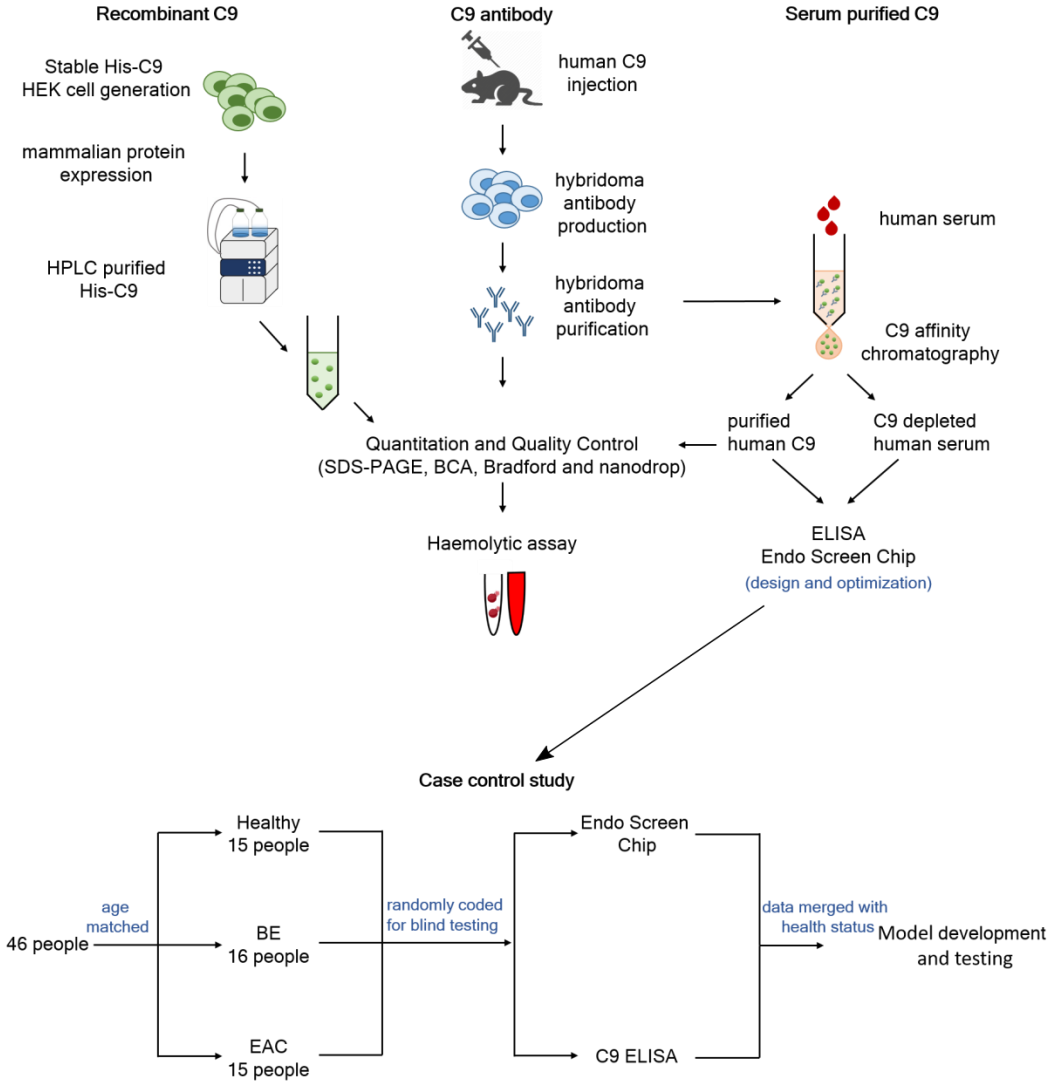

Figure 1. Study overview. High quality reagents including recombinant C9, C9 antibody and serum purified C9 were generated and used to develop C9 ELISA and EndoScreen Chip. The newly established assays were evaluated in a case-control cohort. Logistic regression was used to develop diagnostic algorithms for predicting BE or EAC, by combining blood markers with risk factors.

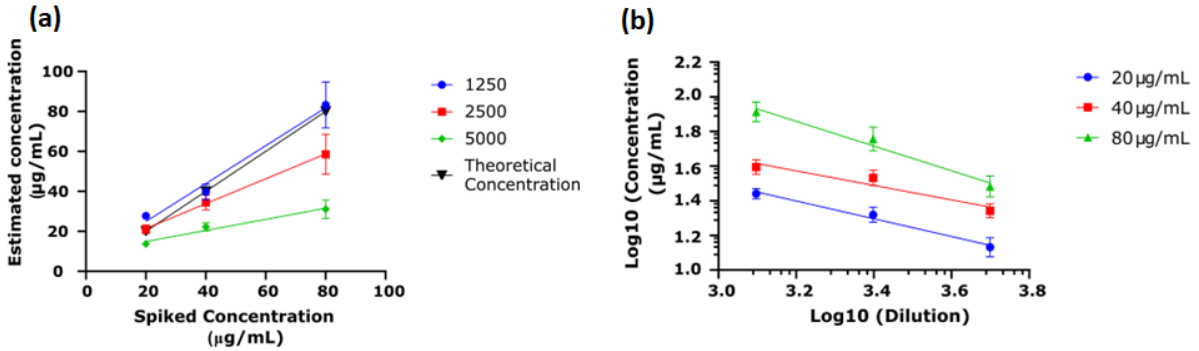

Figure 2. Validation of C9 direct ELISA. His-C9 was expressed and purified for use as the standard, and serum purified C9 was spiked into C9-depleted serum at three concentrations (20 µg/mL, 40 µg/mL and 80 µg/mL). (**a**) Concentration estimated by the ELISA was plotted against the spiked concentration. Dilutions of 1/1250 predicted the theoretical concentration accurately while higher dilutions underestimated the theoretical concentration when samples were spiked at 40 µg/mL and 80 µg/mL (n=3). (**b**) Parallelism was determined by log10 calculation of dilution vs estimated concentration of the spiked sample, demonstrating proportionate estimates of concentration at differing dilutions (n=3).

Preprints (www.preprints.org) | NOT PEER-REVIEWED | Posted: 12 March 2021 doi:10.20944/preprints202103.0330.v1

3.2. Establishing the Endo Screen Chip

Since our original glycoproteomics biomarker pipeline used lectins to assess differentially glycosylated proteins [15], we aimed to develop lectin-immunoassays to measure JAC-C9, one of the top performing biomarkers. However, attempts at lectin-ELISAs were unsuccessful, possibly due to high background and low signal-to-noise ratio [29]. Thus we looked for novel technologies that would allow dual lectin-antibody detection, and had the sensitivity for serum samples. The result was a microfluidic lectin-immune assay for JAC-C9 detection, the EndoScreen Chip (Figure 3A), which integrates highly sensitive nanoparticle barcodes, alternating current electrohydrodynamic (ac-EHD)-induced nanofluidic mixing, and surface-enhanced Raman spectroscopy (SERS). The ac-EHD-induced nanofluidic mixing previously developed by our group [30] acts in nanometer proximity to the JAC-functionalized electrode to: (i) stimulate collisions of JAC-C9 with the sensor surface, (ii) accelerate the binding of the SERS barcodes with the captured JAC-C9, and (iii) reduce sensor fouling through the induced shear forces that remove non-specifically adsorbed non-target molecules. Furthermore, we chose SERS as detection mode due to its high sensitivity, high photo stability of the SERS reporters, and narrow spectral width of the Raman reporter peaks [31].

The EndoScreen Chip consisted of an array of 28 wells to support parallel sample analysis (Figure S2). As depicted in Figure 3A, the asymmetric gold electrodes in each well were functionalized with JAC to capture glycoproteins that bind JAC lectin, including JAC-C9. Subsequent incubation with anti-C9 antibody conjugated SERS nanoparticle barcodes specifically labels the captured JAC-C9 molecules by the C9 protein epitope. The SERS barcodes were also modified with the Raman reporter 5, 5′-dithiobis 2-nitrobenzoic acid (DTNB). Upon laser excitation at 633 nm, DTNB provided a characteristic Raman shift at 1335 cm^{-1}, and its intensity was used for quantification of JAC-C9.

The specificity of EndoScreen Chip was investigated using solutions of 100 ng/ml purified C9 in PBS or in diluted C9-depleted serum (Figure 3B). A strong Raman signal at 1335 cm^{-1} was observed for C9-containing samples, significantly higher than the negligible signals detected in the respective buffer or serum negative controls ($p < 0.01$, t-test, Figure 3B, 3C). Promisingly, the presence of diluted serum matrix caused only a minor suppression on the Raman signal compared to PBS buffer, suggesting the applicability of the assay for clinical sample analysis. Next, we investigated the sensitivity of our assay by using serial dilutions of purified C9 in diluted C9-depleted serum (Figure 3D, 3E). The graphed characteristic Raman peak signals (1335 cm^{-1}) in Figure 3E showed a strong correlation with JAC-C9 concentration (Pearson $R^2 = 0.9835$, $p < 0.0001$). Based on a signal-to-noise ratio of 3, the JAC-C9 detection sensitivity was calculated to be 6.3 ng/mL of spiked purified C9.

Preprints (www.preprints.org) | NOT PEER-REVIEWED | Posted: 12 March 2021 doi:10.20944/preprints202103.0330.v1

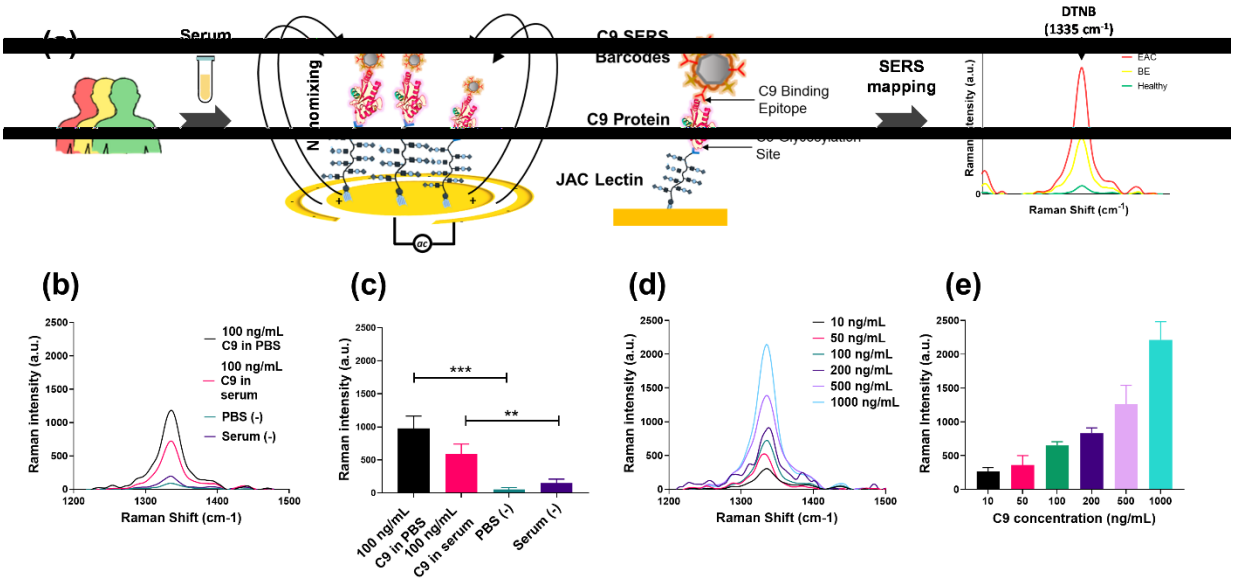

Figure 3. Establishing the EndoScreen Chip. (**a**) Schematic workflow of the chip assay for JAC-C9 detection. JAC-mediated glycoprotein isolation from denatured serum samples and C9 labelling by SERS barcode-tagged anti-C9 antibody is performed under the stimulation of a nanoscopic fluid flow. JAC-C9 is detected by SERS mapping, where the Raman reporter DTNB that is conjugated to the SERS barcodes provides a characteristic Raman peak at 1335 cm-1. (**b**) Raman spectra of 100 ng/mL C9 in PBS (black), 100 ng/mL C9 in diluted serum (pink), blank PBS (cyan), and diluted serum (purple). (**c**) Corresponding averaged Raman signal intensity of DTNB (1335 cm-1). (**d**) Raman spectra and (**e**) averaged Raman signal intensity of DTNB (1335 cm-1) obtained for designated C9 concentrations spiked in diluted serum. The error bars are the standard error of three replicates. **p < 0.01 and ***p < 0.001.

3.3. Total C9 and JAC-C9 are elevated in EAC patient serum

To evaluate the utility of the novel immunoassays as an additional tool for triaging patients for endoscopy, we analyzed a subset of 46 serum samples from the Study of Digestive Health (SDH) [18]. The patients in the SDH study were diagnosed by endoscopy-pathology as BE negative (healthy), BE positive (BE) or EAC positive (EAC). We previously reported elevated serum JAC-C9 in EAC sera in this cohort using multiple reaction monitoring (MRM) mass spectrometry [15], but the total serum C9 level had not yet been analyzed. The selected cohort was matched for age, but differed in heartburn/reflux history, while body mass index (BMI) showed a trend to be higher in EAC (Table S1).

Total serum C9 quantified by ELISA was significantly elevated in EAC compared to BE (one way ANOVA with Tukey's multiple comparisons, $p = 0.0323$, Figure 4A). Consistent with our lectin pulldown coupled mass spectrometry findings [15], EndoScreen Chip analysis revealed elevated levels of serum JAC-C9 in EAC compared to BE (one way ANOVA with Tukey's multiple comparisons, $p = 0.0279$). Although levels of both C9 and JAC-C9 were also increased in EAC compared to healthy, the difference was not statistically significant, possibly due to high variability in the healthy group,

Preprints (www.preprints.org) | NOT PEER-REVIEWED | Posted: 12 March 2021 doi:10.20944/preprints202103.0330.v1

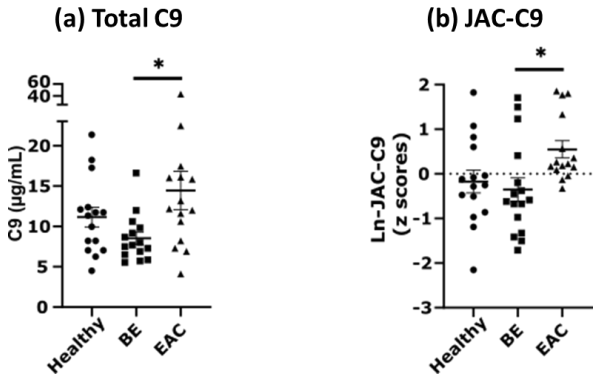

Figure 4. Serum C9 and JAC-C9 are increased in EAC in a cohort of 46 samples. (**a**) Serum C9 concentration was determined using direct ELISA. Patients diagnosed with EAC show significantly increased C9 concentration relative to BE (one way ANOVA with Tukey's multiple comparisons, p = 0.0323). (**b**) JAC-C9 was determined using EndoScreen Chip. Patients diagnosed with EAC show significantly increased JAC-C9 relative to BE (one way ANOVA with Tukey's multiple comparisons, p = 0.0279).

3.4. Serum C9 biomarker panel improves the detection of EAC

Finally, we asked if the EndoScreen Chip and/or the C9 ELISA could be used in conjunction with the known clinical risk factors to improve detection of EAC. Specifically, a simple point-of-care blood biomarker test may help primary care physicians decide which patients are more likely to have EAC or HGD BE, and therefore, be prioritized for endoscopy. Such a blood test could improve the effectiveness of BE surveillance by triaging appropriate patients for endoscopy, and potentially be incorporated into a population screening test for those with risk factors.

To determine the additional value of the novel biomarker panel (JAC-C9 and total C9) above the non-endoscopic clinical risk factors available to the primary care physician, we conducted multinomial logistic regression on the clinical and biomarker data to predict the dependent variables (BE or EAC diagnosis) relative to Healthy. The baseline probability was established by inputting the presenting characteristics of age, BMI and heartburn/reflux history (Table S1) together as a forced forward entry model (Model 1). A second model was then developed by incorporating the blood marker panel data for C9 and JAC-C9 into the baseline model (Model 2, Figure 5, Tables S2, S3). Smoking history was considered; however, at no stage did this contribute significantly to the model, and hence was removed.

Probabilities of correct prediction of disease status from the multinomial logistic regression analysis were visualized as violin plots (Figure 5A). The right shift in the probability of true classification in Model 2 compared to Model 1 showed that the addition of blood biomarkers (Model 2) improved the stratification of patients into correct diagnoses (Figure 5A). The diagnostic ability of the two models was examined by Receiver-operating curve (ROC) analysis for correctly classifying healthy, BE and EAC from the cohort (Figure 5B, Table S4). For all three diagnostic categories, Model 2 increased the area under curve (AUC) relative to Model 1. The AUC for BE classification increased from 0.744 to 0.841, while the AUC for EAC classification increased from 0.838 (Model 1) to 0.931 (Model 2) by addition of the blood biomarker panel. These results demonstrate the utility of incorporating a serum biomarker panel into risk prediction models for BE and EAC.

Preprints (www.preprints.org) | NOT PEER-REVIEWED | Posted: 12 March 2021 doi:10.20944/preprints202103.0330.v1

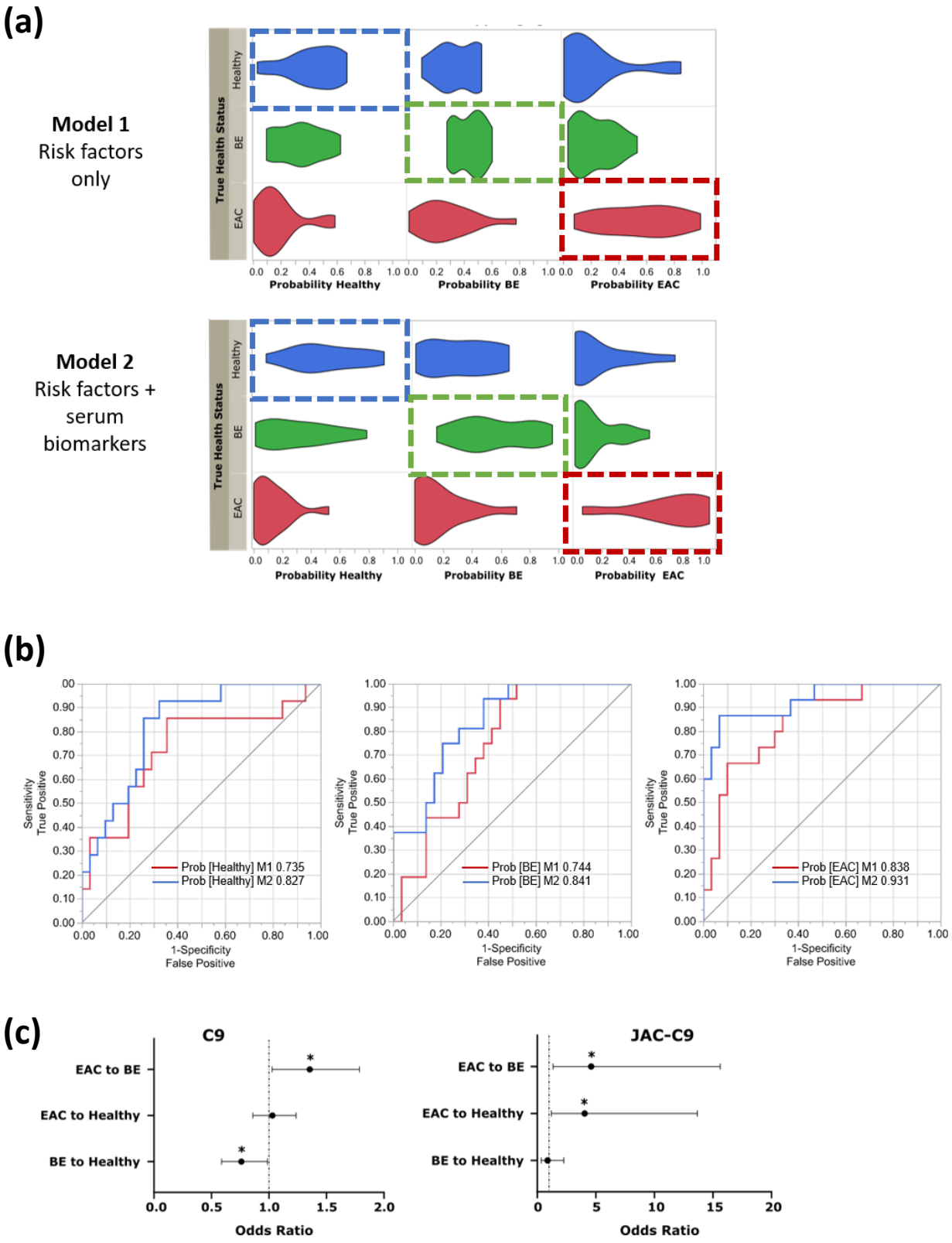

Figure 5. Logistic regression modelling shows improved stratification to true health status. (**a**) Probability outcome plots for patient classified as healthy, BE or EAC, using patient risk factors of BMI, age and heartburn/reflux history alone (Model 1), or patient risk factors plus serum biomarkers C9 and JAC-C9 (Model 2). Probability of health status was plotted as a violin plot against true classification. Boxes indicate the true health status, shift to the right indicates improved classification. (**b**) Receiver operating curve (ROC) for correcting predicting patients as BE or EAC for Model 1 versus Model 2. (**c**) Odds ratios for serum C9 and JAC-C9 in Model 2. C9 shows a significant decrease in BE relative to

Preprints (www.preprints.org) | NOT PEER-REVIEWED | Posted: 12 March 2021 doi:10.20944/preprints202103.0330.v1

healthy, and a significant increase in EAC relative to BE (Wald's test, p <0.05). JAC-C9 shows a significant increase in EAC to healthy and EAC to BE (Wald's test, p<0.05).

Interestingly, although JAC-C9 is a glycoform (subset) of total C9, a paired samples correlation between C9 and JAC-C9 showed that these two variables are not significantly correlated in this dataset (r = 0.119, p = 0.432, n =46). Therefore, we further investigated the contribution of individual markers using odds ratios and Wald statistic (Supplementary Table III, Figure 5C). Both C9 and JAC-C9 contributed significantly to the distinction between EAC and BE, but JAC-C9 had a much higher odds ratio (OR= 4.6; 95% CI: 1.6-15.6; Wald statistic, p = 0.014) compared to total C9 (OR=1.4; 95% CI: 1.0-1.8; Wald statistic, p = 0.032). JAC-C9, but not total C9, contributed to the prediction of EAC relative to healthy (OR=4.1; 95% CI:1.2 - 13.7; Wald statistic, p = 0.024). On the other hand, total C9, but not JAC-C9 contributed to the prediction of BE relative to healthy (Wald statistic, p = 0.039) albeit with a modest odds ratio (OR=0.8; 95% CI: 0.6-1.0). The different diagnostic properties of JAC-C9 and total C9 validate our initial glycoproteomics approach and the development of a glycoform specific JAC-C9 assay.

4. Discussion

Despite the development of risk prediction models and endoscopic surveillance protocols, the ability to diagnose EAC at an earlier stage through screening and surveillance has not appreciably improved over the past decades [4]. On the other hand, the demand for endoscopies is escalating due to population ageing and poor lifestyle factors which lead to gastrointestinal pathologies. Endoscopy is an invasive procedure requiring expert clinicians and significant healthcare resources. A recent Dutch study concluded the overuse of endoscopy surveillance for BE and BE with LGD is associated with substantial costs to the Dutch health system ($53 million per year) for very marginal and uncertain benefits [32]. Moreover, 14% of upper endoscopies in Australian adults offer little benefit and are deemed low-value care [33]. The novel biomarker panel, and in particular the EndoScreen Chip technology reported in this study, have the potential to improve the efficacy and cost-effectiveness of endoscopies when used as a first-line blood test for patients with risk factors of BE and EAC. As demonstrated in the study cohort, the results from the blood marker panel could be used in a risk stratification model with clinical data to determine whether the patient should be prioritized for endoscopic diagnosis of EAC.

A blood biomarker panel test for screening has several advantages which directly address key determinants of the cost-effectiveness of BE screening and surveillance [34]. Blood-based biomarker testing by the primary care physician facilitates triaging of patients along the BE to EAC continuum, improving the diagnostic yield of those that proceed to endoscopy, while decreasing the number of low-yield endoscopies. Additionally, use of an inexpensive liquid biopsy will enable more frequent testing, potentially leading to detection at an earlier stage. Technically, the use of a blood marker panel may reduce the high variability of biopsy-based early stage BE and low grade dysplasia (LGD) diagnoses, which rely on the experience of the pathologist [7]. From the patient and compliance viewpoint, blood testing is familiar and commonly accepted. Indeed, a recent survey of 554 Dutch population respondents returned a strong preference of non-invasive (blood or breath) tests over endoscopic or capsule-based tests, provided the test is sufficiently sensitive [35]. Furthermore, a single blood draw may be used for multiple blood tests in the pathology laboratory. As older age increases the risk of multiple cancers, a routine blood draw for pan-cancer risk stratification is an attractive option. The feasibility of a blood test for cancer screening was recently confirmed by a large, multi-center trial with > 9,900 participants baseline tested using the multi-analyte CancerSEEK blood test, with positive cases followed by positron emission tomography–computed tomography (PET-CT) for diagnosis and localization of the cancer, if present [36]. In our scenario, detection

Preprints (www.preprints.org) | NOT PEER-REVIEWED | Posted: 12 March 2021 doi:10.20944/preprints202103.0330.v1

of high risk patients using C9 ELISA and EndoScreen Chip will be followed with endoscopic diagnosis and treatment if required.

The goal of C9 ELISA/EndoScreen Chip and BE surveillance programs are to detect early stage EAC, and dysplastic BE. This contrasts with the newly developed BE tests such as the Cytosponge, EsophaCap and EsoCheck, which aim to detect BE. As 90% of EAC patients do not have prior BE diagnosis, and therefore are not in a routine endoscopic surveillance program [3], the ability of the C9 ELISA/EndoScreen Chip test to distinguish EAC from healthy, as well as BE patients, makes it suitable as a first-line screening tool. While the current proof of concept study did not include early cancer samples, our panel of glycoprotein biomarkers, including JAC-C9 and 3 other glycoforms of C9, were previously validated to detect high grade dysplasia and EAC in two independent cohorts [16]. These serum glycoproteins are, to our knowledge, rather unique in their ability to detect dysplasia. In contrast, the selected serum protein and cell free tumor DNA panel in CancerSEEK, and a more recent study using cell-free DNA methylation signature both reported poor sensitivity for Stage 1 esophageal cancer, at around 20% [37,38]. Hence, our alternative approach targeting protein glycosylation in serum proteins is complementary to nucleic acid-based liquid biopsies, and may be more useful for early cancer, including dysplasia detection.

Complement component 9 (C9) is a circulating glycoprotein with complex glycosylation patterns [39]. In addition to our work in EAC, proteomic and glycoproteomic cancer biomarker discovery studies have reported plasma/serum C9 as a biomarker for colorectal cancer, gastric cancer, squamous cell lung cancer and glioblastoma [40-43]. While we have confirmed elevated C9 glycoforms in multiple EAC cohorts using lectin-pulldown-coupled quantitative mass spectrometry [15,16], this is the first report of elevated total serum C9 in EAC, and additional EAC cohort evaluation for total serum C9 is required. Nevertheless, the multiple independent reports of elevated serum C9 or glycoforms of C9 in multiple cancers support the mounting evidence for complement system dysregulation in cancer [44].

In the present cohort, we found that JAC-C9 has a much higher odds ratio for EAC compared to total C9, which affirms the sub-proteome approach to biomarker discovery. We focused on glycoproteins and chose lectin as an affinity agent, because the results could be readily translated to lectin immunoassays. To overcome the high background, and low sensitivity observed with a conventional lectin-ELISA, we devised a microfluidic chip strategy – the EndoScreen Chip. An electric field induced nanoscopic fluid flow in proximity to the surface-immobilized JAC was employed to remove weakly bound molecules, while signal enhancement by localized surface plasmon resonance allows highly sensitivity detection. Working synergistically, the nanofluidic mixing and SERS read-out were instrumental to the achieved limit of detection (6.3 ng/ml) from 2 µL of serum per patient. The EndoScreen Chip can be expanded to multiplex a panel of glycoproteins, either by using additional antibodies with different SERS tags to detect other JAC-binding protein biomarkers (which are present in our panel), or by adding other lectins to the other channels, for detection with C9, or other antibodies. Each of the new biomarker lectin-immunoassays will need to be separately validated prior to multiplexing.

Several limitations of the current study need to be acknowledged. Firstly, we used only two biomarkers, JAC-C9 and total C9, in our proof-of-concept biomarker panel. While our glycoproteomics pipeline generated a number of validated serum glycoprotein biomarkers for early EAC [16,45], translation to immunoassays requires the generation of high quality antibodies and standard proteins which can be a bottle neck for novel biomarkers. Secondly, we evaluated the biomarker panel in a single cohort of 46 participants, distributed evenly between three conditions (healthy, BE and EAC). As the proportion of BE and EAC in our cohort is much higher than the population prevalence (1-2% BE, <1% progression to EAC [7]), the predictive ability may prove to be lower in larger, more representative cohorts [46]. External validation of the serum biomarker-assisted predictive algorithm on additional cohorts with dysplastic BE patients will be required, while

development and multiplexing of additional blood-based biomarkers may further increase the precision of BE/EAC prediction. Finally, the exact glycosylation structures recognized by JAC on C9, and how it is altered during BE-EAC development, remain to be elucidated.

5. Conclusions

In conclusion, serum Complement C9 immunoassays and particularly the novel microfluidic pre-endoscopy blood biomarker EndoScreen Chip test have the potential to transform BE management and EAC detection. Although development of a multiplexed panel and clinical trials are still needed, ultimately, the ability to stratify patients for EAC risk based on blood markers and clinical risk factors will increase patient compliance in screening programs and allow the most effective utilization of endoscopy resources.

Supplementary Materials: The following are available online at www.mdpi.com/xxx/s1, Figure S1: Production and purification of C9 and antibody, Figure S2: Endo Screen Chip design and functionalization, Table S1: Patient risk factors, Table S2: Comparison of disease classification by each model, Table S3: Properties of model 2, Table S4: Confidence intervals for multinomial logistic regression.

Author Contributions: Conceptualization, Julie Webster, Alain Wuethrich, Alok Shah, Matt Trau and Michelle Hill; Formal analysis, Julie Webster and Gunter Hartel; Funding acquisition, Alain Wuethrich and Matt Trau; Investigation, Julie Webster, Alain Wuethrich and Karthik Shanmugasundaram; Methodology, Julie Webster, Alain Wuethrich and B. Morgan; Resources, Renee Richards, Wioleta Zelek and B. Morgan; Supervision, Michelle Hill; Visualization, Julie Webster, Alain Wuethrich and Gunter Hartel; Writing – original draft, Julie Webster and Michelle Hill; Writing – review & editing, Renee Richards, Louisa Gordon, Bradley Kendall and Michelle Hill.

Funding: This research was funded by National Foundation for Medical Research and Innovation (to MMH). The Study of Digestive Health was supported by grant number 5 RO1 CA 001833-02 from the National Cancer Institute. The contents of this paper are solely the responsibility of the authors and do not necessarily represent the official views of the National Cancer Institute. We thank the National Breast Cancer Foundation of Australia (CG-12-07), Australian Research Council (DP210103151), and National Health and Medical Research Council (APP1173669) for supporting MT and AW.

Institutional Review Board Statement: The study was conducted according to the guidelines of the Declaration of Helsinki, and approved by the Human Research Ethics Committee of QIMR Berghofer Medical Research Institute (project number P2352).

Informed Consent Statement: Informed consent was obtained from all subjects involved in the study.

Acknowledgments: We thank Associate Professor Michelle Dunston (Monash University, Melbourne, Australia) for providing the mammalian C9 expression plasmid, and Dr Bradley Spicer (Monash University, Melbourne, Australia) for discussions. The device fabrication and Raman measurement were conducted at Queensland node of the Australian National Fabrication Facility (Q-ANFF).

Conflicts of Interest: MMH and AKS are inventors on a patent entitled "Glycoprotein biomarkers for esophageal adenocarcinoma and Barrett's esophagus and uses thereof." The funders had no role in the design of the study; in the collection, analyses, or interpretation of data; in the writing of the manuscript, or in the decision to publish the results.

References

1. Inadomi, J.M.; Saxena, N. Screening and Surveillance for Barrett's Esophagus: Is It Cost-Effective? *Dig Dis Sci* **2018**, *63*, 2094-2104, doi:10.1007/s10620-018-5148-7.
2. Souza, R.F.; Spechler, S.J. Advances in Biomarkers for Risk Stratification in Barrett's Esophagus. *Gastrointest Endosc Clin N Am* **2021**, *31*, 105-115, doi:10.1016/j.giec.2020.08.007.
3. Tan, W.K.; Sharma, A.N.; Chak, A.; Fitzgerald, R.C. Progress in Screening for Barrett's Esophagus: Beyond Standard Upper Endoscopy. *Gastrointest Endosc Clin N Am* **2021**, *31*, 43-58, doi:10.1016/j.giec.2020.08.004.
4. Thrift, A.P. Barrett's Esophagus and Esophageal Adenocarcinoma: How Common Are They Really? *Digestive Diseases and Sciences* **2018**, *63*, 1988-1996, doi:10.1007/s10620-018-5068-6.

5. Ireland, C.J.; Thrift, A.P.; Esterman, A. Risk Prediction Models for Barrett's Esophagus Discriminate Well and Are Generalizable in an External Validation Study. *Dig Dis Sci* **2020**, *65*, 2992-2999, doi:10.1007/s10620-019-06018-2.
6. Rubenstein, J.H.; Morgenstern, H.; Appelman, H.; Scheiman, J.; Schoenfeld, P.; McMahon, L.F., Jr.; Metko, V.; Near, E.; Kellenberg, J.; Kalish, T., et al. Prediction of Barrett's esophagus among men. *Am J Gastroenterol* **2013**, *108*, 353-362, doi:10.1038/ajg.2012.446.
7. Wani, S.; Rubenstein, J.H.; Vieth, M.; Bergman, J. Diagnosis and Management of Low-Grade Dysplasia in Barrett's Esophagus: Expert Review From the Clinical Practice Updates Committee of the American Gastroenterological Association. *Gastroenterology* **2016**, *151*, 822-835, doi:https://doi.org/10.1053/j.gastro.2016.09.040.
8. Rosenfeld, A.; Graham, D.G.; Jevons, S.; Ariza, J.; Hagan, D.; Wilson, A.; Lovat, S.J.; Sami, S.S.; Ahmad, O.F.; Novelli, M., et al. Development and validation of a risk prediction model to diagnose Barrett's oesophagus (MARK-BE): a case-control machine learning approach. *Lancet Digit Health* **2020**, *2*, E37-e48, doi:10.1016/s2589-7500(19)30216-x.
9. Thrift, A.P. Barrett's Esophagus and Esophageal Adenocarcinoma: How Common Are They Really? *Digestive diseases and sciences* **2018**, *63*, 1988-1996, doi:10.1007/s10620-018-5068-6.
10. Coleman, H.G.; Xie, S.-H.; Lagergren, J. The Epidemiology of Esophageal Adenocarcinoma. *Gastroenterology* **2018**, *154*, 390-405, doi:10.1053/j.gastro.2017.07.046.
11. Cook, M.B.; Thrift, A.P. Epidemiology of Barrett's Esophagus and Esophageal Adenocarcinoma: Implications for Screening and Surveillance. *Gastrointest Endosc Clin N Am* **2021**, *31*, 1-26, doi:10.1016/j.giec.2020.08.001.
12. Grady, W.M.; Yu, M.; Markowitz, S.D.; Chak, A. Barrett's Esophagus and Esophageal Adenocarcinoma Biomarkers. *Cancer Epidemiol Biomarkers Prev* **2020**, *29*, 2486-2494, doi:10.1158/1055-9965.EPI-20-0223.
13. Shah, A.K.; Saunders, N.A.; Barbour, A.P.; Hill, M.M. Early diagnostic biomarkers for esophageal adenocarcinoma--the current state of play. *Cancer Epidemiol Biomarkers Prev* **2013**, *22*, 1185-1209, doi:10.1158/1055-9965.EPI-12-1415.
14. Choi, E.; Loo, D.; Dennis, J.W.; O'Leary, C.A.; Hill, M.M. High-throughput lectin magnetic bead array-coupled tandem mass spectrometry for glycoprotein biomarker discovery. *Electrophoresis* **2011**, *32*, 3564-3575, doi:10.1002/elps.201100341.
15. Shah, A.K.; Cao, K.A.; Choi, E.; Chen, D.; Gautier, B.; Nancarrow, D.; Whiteman, D.C.; Saunders, N.A.; Barbour, A.P.; Joshi, V., et al. Serum Glycoprotein Biomarker Discovery and Qualification Pipeline Reveals Novel Diagnostic Biomarker Candidates for Esophageal Adenocarcinoma. *Mol Cell Proteomics* **2015**, *14*, 3023-3039, doi:10.1074/mcp.M115.050922.
16. Shah, A.K.; Hartel, G.; Brown, I.; Winterford, C.; Na, R.; Cao, K.L.; Spicer, B.A.; Dunstone, M.A.; Phillips, W.A.; Lord, R.V., et al. Evaluation of Serum Glycoprotein Biomarker Candidates for Detection of Esophageal Adenocarcinoma and Surveillance of Barrett's Esophagus. *Mol Cell Proteomics* **2018**, *17*, 2324-2334, doi:10.1074/mcp.RA118.000734.
17. Nancarrow, D.J.; Clouston, A.D.; Smithers, B.M.; Gotley, D.C.; Drew, P.A.; Watson, D.I.; Tyagi, S.; Hayward, N.K.; Whiteman, D.C.; for the Australian Cancer, S., et al. Whole Genome Expression Array Profiling Highlights Differences in Mucosal Defense Genes in Barrett's Esophagus and Esophageal Adenocarcinoma. *PLOS ONE* **2011**, *6*, e22513, doi:10.1371/journal.pone.0022513.
18. Smith, K.J.; O'Brien, S.M.; Smithers, B.M.; Gotley, D.C.; Webb, P.M.; Green, A.C.; Whiteman, D.C. Interactions among smoking, obesity, and symptoms of acid reflux in Barrett's esophagus. *Cancer Epidemiol Biomarkers Prev* **2005**, *14*, 2481-2486, doi:10.1158/1055-9965.Epi-05-0370.
19. Dudkina, N.V.; Spicer, B.A.; Reboul, C.F.; Conroy, P.J.; Lukoyanova, N.; Elmlund, H.; Law, R.H.P.; Ekkel, S.M.; Kondos, S.C.; Goode, R.J.A., et al. Structure of the poly-C9 component of the complement membrane attack complex. *Nature Communications* **2016**, *7*, 10588, doi:10.1038/ncomms10588 https://www.nature.com/articles/ncomms10588#supplementary-information.
20. Köhler, G.; Milstein, C. Continuous cultures of fused cells secreting antibody of predefined specificity. *Nature* **1975**, *256*, 495-497, doi:10.1038/256495a0.
21. Morgan, B.P. Immunoaffinity Methods for Purification of Complement Components and Regulators. In *Complement Methods and Protocols. Methods in Molecular Biology*, Morgan, B.P., Ed. Humana Press Inc.: Totowa, NJ, 2000; https://doi.org/10.1385/1-59259-056-X:53.
22. Zelek, W.M.; Harris, C.L.; Morgan, B.P. Extracting the barbs from complement assays: Identification and optimisation of a safe substitute for traditional buffers. *Immunobiology* **2018**, *223*, 744-749, doi:10.1016/j.imbio.2018.07.016.
23. Zhang, Z.; Wang, J.; Shanmugasundaram, K.B.; Yeo, B.; Möller, A.; Wuethrich, A.; Lin, L.L.; Trau, M. Tracking Drug-Induced Epithelial–Mesenchymal Transition in Breast Cancer by a Microfluidic Surface-Enhanced Raman Spectroscopy Immunoassay. *Small* **2020**, *16*, 1905614, doi:10.1002/smll.201905614.
24. Frens, G. Controlled Nucleation for the Regulation of the Particle Size in Monodisperse Gold Suspensions. *Nature Physical Science* **1973**, *241*, 20-22, doi:10.1038/physci241020a0.
25. Zhao, J.; Lui, H.; McLean, D.I.; Zeng, H. Automated Autofluorescence Background Subtraction Algorithm for Biomedical Raman Spectroscopy. *Appl. Spectrosc.* **2007**, *61*, 1225-1232.
26. Fenlon, C.; O'Grady, L.; Doherty, M.L.; Dunnion, J. A discussion of calibration techniques for evaluating binary and categorical predictive models. *Preventive Veterinary Medicine* **2018**, *149*, 107-114, doi:https://doi.org/10.1016/j.prevetmed.2017.11.018.
27. FDA, U. Q2 (R1) Validation of Analytical Procedures: Text and Methodology. Availabe online: https://www.fda.gov/regulatory-information/search-fda-guidance-documents/q2-r1-validation-analytical-procedures-text-and-methodology
28. Andreasson, U.; Perret-Liaudet, A.; van Waalwijk van Doorn, L.J.C.; Blennow, K.; Chiasserini, D.; Engelborghs, S.; Fladby, T.; Genc, S.; Kruse, N.; Kuiperij, H.B., et al. A Practical Guide to Immunoassay Method Validation. *Front Neurol* **2015**, *6*, 179-179, doi:10.3389/fneur.2015.00179.

29. Thompson, R.; Creavin, A.; O'Connell, M.; O'Connor, B.; Clarke, P. Optimization of the enzyme-linked lectin assay for enhanced glycoprotein and glycoconjugate analysis. *Analytical biochemistry* **2011**, *413*, 114-122, doi:10.1016/j.ab.2011.02.013.
30. Khondakar, K.R.; Dey, S.; Wuethrich, A.; Sina, A.A.I.; Trau, M. Toward Personalized Cancer Treatment: From Diagnostics to Therapy Monitoring in Miniaturized Electrohydrodynamic Systems. *Accounts of Chemical Research* **2019**, *52*, 2113-2123, doi:10.1021/acs.accounts.9b00192.
31. Ding, S.-Y.; Yi, J.; Li, J.-F.; Ren, B.; Wu, D.-Y.; Panneerselvam, R.; Tian, Z.-Q. Nanostructure-based plasmon-enhanced Raman spectroscopy for surface analysis of materials. *Nature Reviews Materials* **2016**, *1*, 16021, doi:10.1038/natrevmats.2016.21.
32. Cotton, C.C.; Shaheen, N.J. Overutilization of Endoscopic Surveillance in Barrett's Esophagus: The Perils of Too Much of a Good Thing. *Am J Gastroenterol* **2020**, *115*, 1019-1021, doi:10.14309/ajg.0000000000000650.
33. Care, A.C.o.S.a.Q.i.H. Third Australian Atlas of Healthcare Variation 2018. Availabe online: https://www.safetyandquality.gov.au/our-work/healthcare-variation/third-atlas-2018
34. Hirst, N.G.; Gordon, L.G.; Whiteman, D.C.; Watson, D.I.; Barendregt, J.J. Is endoscopic surveillance for non-dysplastic Barrett's esophagus cost-effective? Review of economic evaluations. *Journal of Gastroenterology and Hepatology* **2011**, *26*, 247-254, doi:10.1111/j.1440-1746.2010.06506.x.
35. Peters, Y.; Siersema, P.D. Public Preferences and Predicted Uptake for Esophageal Cancer Screening Strategies: A Labeled Discrete Choice Experiment. *Clin Transl Gastroenterol* **2020**, *11*, e00260, doi:10.14309/ctg.0000000000000260.
36. Lennon, A.M.; Buchanan, A.H.; Kinde, I.; Warren, A.; Honushefsky, A.; Cohain, A.T.; Ledbetter, D.H.; Sanfilippo, F.; Sheridan, K.; Rosica, D., et al. Feasibility of blood testing combined with PET-CT to screen for cancer and guide intervention. *Science* **2020**, *369*, doi:10.1126/science.abb9601.
37. Cohen, J.D.; Li, L.; Wang, Y.; Thoburn, C.; Afsari, B.; Danilova, L.; Douville, C.; Javed, A.A.; Wong, F.; Mattox, A., et al. Detection and localization of surgically resectable cancers with a multi-analyte blood test. *Science* **2018**, *359*, 926-930, doi:10.1126/science.aar3247.
38. Liu, M.C.; Oxnard, G.R.; Klein, E.A.; Swanton, C.; Seiden, M.V.; Consortium, C. Sensitive and specific multi-cancer detection and localization using methylation signatures in cell-free DNA. *Annal Onc* **2020**, *31*, 745-759.
39. Franc, V.; Yang, Y.; Heck, A.J. Proteoform Profile Mapping of the Human Serum Complement Component C9 Revealing Unexpected New Features of N-, O-, and C-Glycosylation. *Anal Chem* **2017**, *89*, 3483-3491, doi:10.1021/acs.analchem.6b04527.
40. Chong, P.K.; Lee, H.; Loh, M.C.; Choong, L.Y.; Lin, Q.; So, J.B.; Lim, K.H.; Soo, R.A.; Yong, W.P.; Chan, S.P., et al. Upregulation of plasma C9 protein in gastric cancer patients. *Proteomics* **2010**, *10*, 3210-3221, doi:10.1002/pmic.201000127.
41. Miyauchi, E.; Furuta, T.; Ohtsuki, S.; Tachikawa, M.; Uchida, Y.; Sabit, H.; Obuchi, W.; Baba, T.; Watanabe, M.; Terasaki, T., et al. Identification of blood biomarkers in glioblastoma by SWATH mass spectrometry and quantitative targeted absolute proteomics. *PLoS One* **2018**, *13*, e0193799, doi:10.1371/journal.pone.0193799.
42. Murakoshi, Y.; Honda, K.; Sasazuki, S.; Ono, M.; Negishi, A.; Matsubara, J.; Sakuma, T.; Kuwabara, H.; Nakamori, S.; Sata, N., et al. Plasma biomarker discovery and validation for colorectal cancer by quantitative shotgun mass spectrometry and protein microarray. *Cancer Sci* **2011**, *102*, 630-638, doi:10.1111/j.1349-7006.2010.01818.x.
43. Narayanasamy, A.; Ahn, J.M.; Sung, H.J.; Kong, D.H.; Ha, K.S.; Lee, S.Y.; Cho, J.Y. Fucosylated glycoproteomic approach to identify a complement component 9 associated with squamous cell lung cancer (SQLC). *J Proteomics* **2011**, *74*, 2948-2958, doi:10.1016/j.jprot.2011.07.019.
44. Thurman, J.M.; Laskowski, J.; Nemenoff, R.A. Complement and Cancer-A Dysfunctional Relationship? *Antibodies (Basel)* **2020**, *9*, doi:10.3390/antib9040061.
45. Shah, A.K.; Le Cao, K.A.; Choi, E.; Chen, D.; Gautier, B.; Nancarrow, D.; Whiteman, D.C.; Baker, P.R.; Clauser, K.R.; Chalkley, R.J., et al. Glyco-centric lectin magnetic bead array (LeMBA) - proteomics dataset of human serum samples from healthy, Barretts esophagus and esophageal adenocarcinoma individuals. *Data Brief* **2016**, *7*, 1058-1062, doi:10.1016/j.dib.2016.03.081.
46. Thrift, A.P.; Kanwal, F.; El-Serag, H.B. Prediction Models for Gastrointestinal and Liver Diseases: Too Many Developed, Too Few Validated. *Clinical Gastroenterology and Hepatology* **2016**, *14*, 1678-1680, doi:10.1016/j.cgh.2016.08.026.